[Article ID] 1003- 6326(2002)02- 0183- 06

UBET analysis of process of extruding aluminum alloy ribbed thin-wall pipes through a porthole die[①]

XIE Jian-xin(谢建新)[1], PEI Qiang(裴 强)[1], LIU Jing-an(刘静安)[2]
(1. Materials Science and Engineering School, University of Science and Technology Beijing, Beijing 100083, China;
2. Southwest Aluminum Fabrication Plant, Chongqing 401326, China)

[Abstract] Using the upper bound element technique (UBET), a numerical model was proposed for analyzing the metal deformation behavior in the extrusion process of ribbed thin-wall pipes through a porthole die. Optimization parameters were contained in the numerical model and determined through minimizing the total work of metal deformation. Taking the extrusion process of thin-wall pipe with one rib as an example, the calculated results using the proposed model are as follows: the extrusion pressure p is linearly related to the extrusion ratio R by $p = a + bR^{0.683}$, where $a = 14.13$, $b = 0.911$. When the length of the billet remaining in container is shorter than a quarter of the container diameter, the plastic region extends over the whole of the remained billet and the extrusion process reaches the state of funnel deformation. There exists an optimum depth of welding chamber in respect of the extrusion pressure, and to the calculated example the optimum depth is about 10% of the circumscribed diameter of portholes. To obtain more equitable metal flow in welding chamber, it is required to make the dividing planes in container to be consistent with corresponding welding planes in the chamber ($\theta_{\max i} = \theta'_{\max i}$) through choosing different entering area for each of the portholes.

[Key words] ribbed tube; extrusion; upper bound element technique; porthole die; die design
[CLC number] TG 376.2 **[Document code]** A

1 INTRODUCTION

A kind of thin-wall pipe with one or several ribs on the outer circumference, so-called ribbed thin-wall pipe, is widely used in petroleum, chemical, transportation and aviation industries. Fig. 1 shows a kind of thin-wall pipe with one rib used as buoyancy pipe in large oil depot. Because its poor symmetry and thin-wall compared to the contour dimension, this kind of pipe is difficult to manufacture and is usually extruded through a porthole die. The reasonable die-design is the key to ensure successful production and to improve pipe quality. But in present situation, the extrusion pressure required by extruding this kind pipe is estimated by simple experiential formula, the die-design is depended on the experiences and the designed die needs to be testified by experiment which may cause waste of manpower and material resource[1~4]. In view of this situation, a numerical model based on Upper Bound Elemental Technique (UBET)[5] is proposed to analyze the extrusion process of ribbed thin-wall pipe through a porthole die, which being helpful in the optimization of die-design and extrusion pressure calculation in practical extrusion process of ribbed thin-wall pipes.

2 NUMERICAL MODEL

The numerical model built in this paper can be applied to analyze the extrusion process of thin-wall pipe with one or several ribs through a porthole die which may has different dimensions and different number of fan portholes. For simplicity and convenience, the die with four fan portholes shown in Fig. 2 is taken as an example to explain the numerical model.

2.1 Geometrical description of plastic regions

Early investigation results[6~8] show that the deformation in porthole die extrusion can be supposed to consist of two processes, one being the dividing pro-

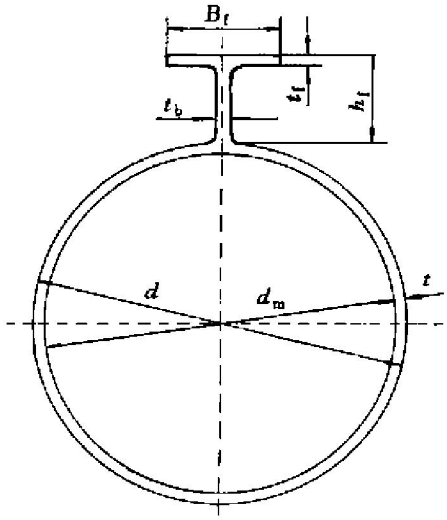

Fig. 1 Ribbed thin-wall pipe

① [Received date] 2001- 08- 23; [Accepted date] 2001- 11- 19

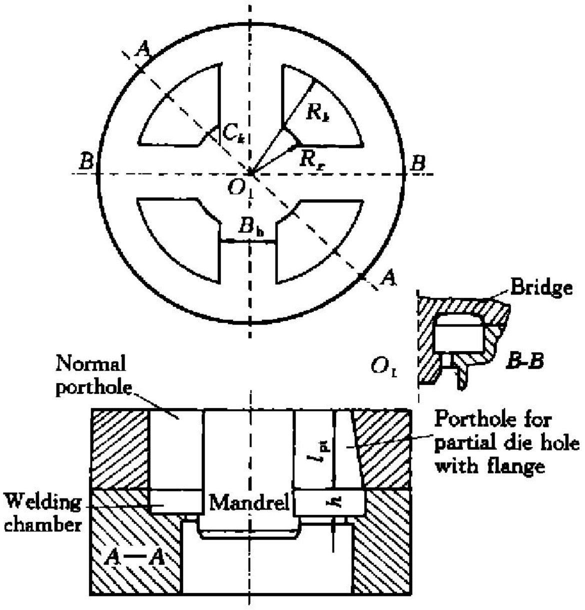

Fig. 2 Scheme of porthole die for thin-wall ribbed pipe extrusion

cess in which the billet is dividing into several bars by the bridge, and the other being the welding process in which the divided bars are welded together again and required product is formed. According to general characteristics of porthole die extrusion and combining with specific status of the research objective in this paper, the metal flow models in dividing and welding process are established, as shown in Fig. 3 and Fig. 4. Fig. 3(c) shows the shapes of the plastic and dead metal regions on hoop plane over the bridge. The elements under the bridge are divided as the same as those over the bridge.

In the following derivation about velocity field, cylindrical coordinates are employed and axial coordinate between the dividing and the welding process is distinguished by z_1 and z_2 respectively, whilist symbol z without subscript denotes that the expression is the same as the two processes. As shown in Fig. 3 and Fig. 4, the plane of O_1A is axial symmetrical plane of portholes and O_1B being axial symmetrical plane of bridge. The planes on which dividing of the billet or welding of the divided bars takes place are uncertain of consistent with the plane O_1B, their positions are determined by parameters $\theta_{\max i}$ and $\theta'_{\max i}$ ($i = 1, 2, 3, 4$). $\theta_{\max i}$ and $\theta'_{\max i}$ as well as r_p, h_n, H_n ($n = 1, 2, 3, 4$) are determined by minimizing the total work of deformation in the process, so-called optimization parameters. θ_{pi}, θ_o, θ_1, C_1, C_2 are constants determined by die dimension.

2.2 Kinematically admissible velocity field

The plastic regions are divided into elements whose discontinuous velocity along tangent direction may exit but the vertical velocity must be continuous on the boundaries. In every element, however, the velocity field is continuous.

2.2.1 Velocity field in elements

On the basis of geometrical model of plastic region, every deformation region is individually divided into two types of elements by thin lines as shown in Fig. 3 and Fig. 4. As shown in Fig. 5, one kind of the elements with a rectangle shape in axial-section plane is called rectangular element, and the other with a triangular shape in axial-section plane is called trian-

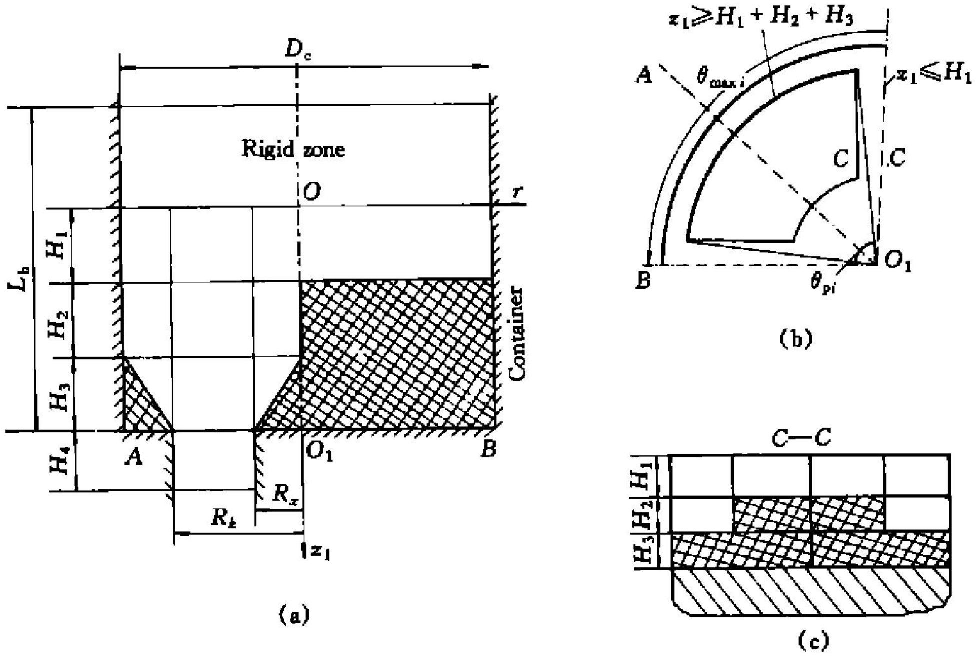

Fig. 3 Geometric shape diagram of dividing deformation region

(a) —Shape of dividing deformation region on symmetrical planes of O_1A and O_1B (refer to Fig. 2);

(b) —Shape of dividing deformation region on typical cross sections corresponded to porthole;

(c) —Shape of plastic and dead metal regions on hoop plane over bridge

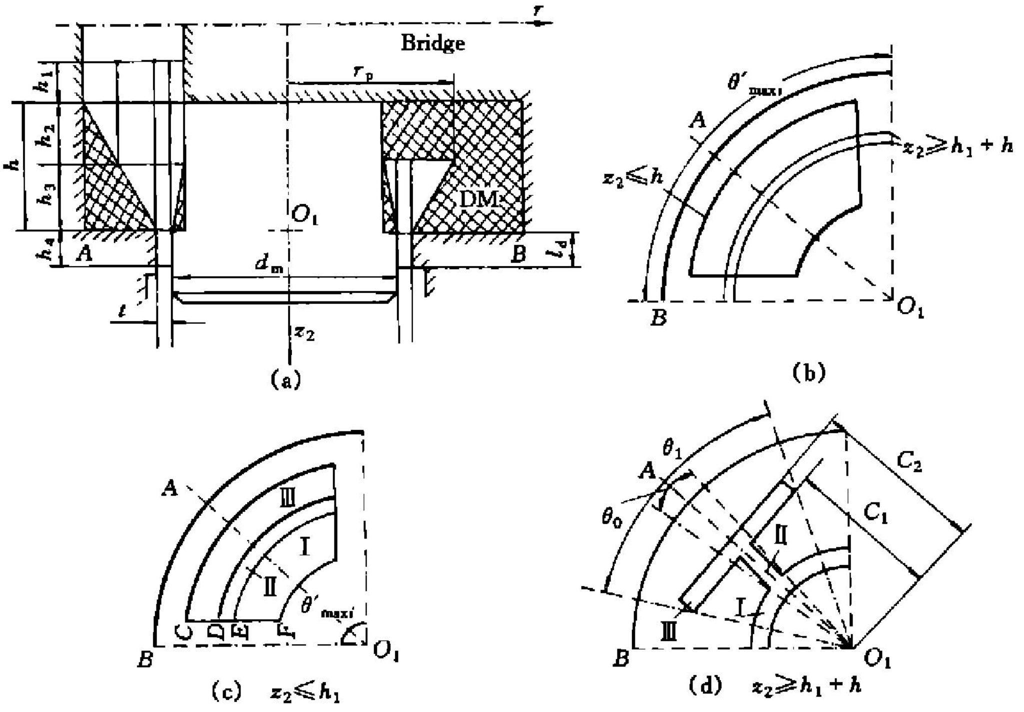

Fig. 4 Geometric shape diagram of welding deformation region
(a) —Shape of welding deformation region on symmetrical planes of O_1A and O_1B corresponded to round part of pipe (refer to Fig. 2); (b) —Shape of welding deformation region on typical cross sections corresponded to a porthole; (c), (d) —Showing metal flow relationship in porthole and in die hole corresponded to ribbed part of pipe

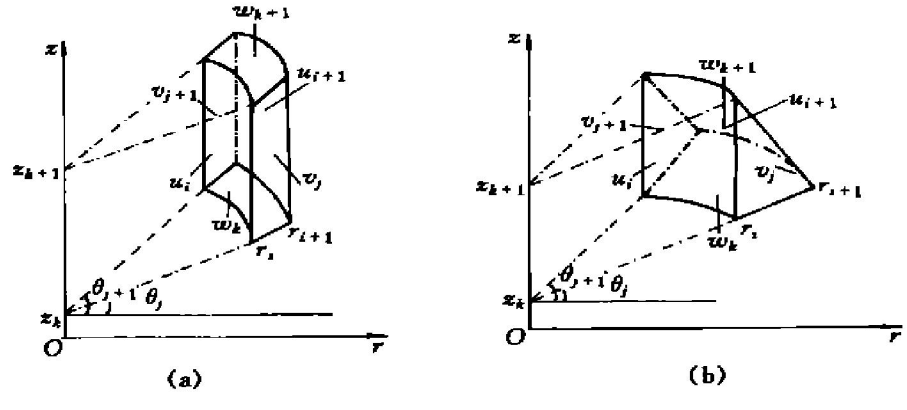

Fig. 5 Rectangle and triangle elements
(a) —Rectangle element; (b) —Triangle element

gle element.

In cylindrical coordinates, three velocity subdivision of a random point in an element are assumed to be u, v, w. Employing volume-consistancy condition shown by

$$\dot{\varepsilon}_r + \dot{\varepsilon}_\theta + \dot{\varepsilon}_z = 0 \qquad (1)$$

and element velocity boundary conditions, a three-dimensional kinematically admissible velocity may be established in two types elements. Axial plane assumption is taken in rectangle elements and circumferential plane assumption in triangle elements. The velocity subdivisions are described as follows:

In rectangle element

$$w = a_1 z + a_2 \qquad (2a)$$

$$u = r f_1(\theta)/2 + a_3/r \qquad (2b)$$

$$v = -r\int f_1(\theta)\mathrm{d}\theta - a_1 r\theta + f_2(\theta) \qquad (2c)$$

In triangle element

$$w = z g_1(r) + g_2(r) \qquad (3a)$$

$$u = -\frac{1}{r}\left[\int g_1(r) r \mathrm{d}r + a_4 r + k(z)\right] \qquad (3b)$$

$$v = a_4\theta + a_5 \qquad (3c)$$

where $f_1(\theta)$, $f_2(\theta)$, $g_1(r)$, $g_2(r)$, $k(z)$, are functions determined, a_1, a_2, a_3, a_4, a_5, are parameters determined by velocity boundary conditions of elements.

2.2.2 Vertical velocity on element boundary planes

According to UBET theorem, vertical velocities on element boundaries are assumed to distribute evenly, thus the vertical velocity of the center point of the boundary may be used to describe that on the whole boundary. The vertical velocity of the center point is a function of the coordination (position of the element). The vertical velocity subdivision w of the boundary's center point can be assumed as following:

$$w(r, \theta, z) = \frac{F_0 v_0}{\int_{F_z} q_z(r, \theta) \mathrm{d} F_z} q_z(r, \theta) = \frac{F_0 v_0}{\sum_{r, \theta, z} q_z(r, \theta) F_z(r, \theta)} q_z(r, \theta) \tag{4}$$

where F_0 is the cross-sectional area of the container, v_0 is velocity of extrusion ram, $F_z(r, \theta)$ is cross-sectional area of (i, j) element of kth layer (i, j, k represent sequence number of r, θ, z coordinates respectively), $q_z(r, \theta)$ are the functions describing vertical velocity distribution of the boundary's center point between number k and $k+1$ layers. Considering the shape of deformation region and the boundary conditions, $q_z(r, \theta)$ can be given by

$$q_z(r, \theta) = \left[(r_{\max} - r)\frac{r}{r_{\max}}\right]^{a_6}(1 + a_7\theta) \tag{5}$$

where $r_{\max}$ denotes the outer boundary's coordinate of plastic region; a_6, a_7 are optimization parameters determined through minimizing the total work of deformation in the process.

The vertical velocity subdivision u, v of the boundary's center point of elements can be determined by

$$2\frac{v_{i,j,k} - v_{i,j,k}}{(r_{i+1} + r_i)(\theta_{j+1} - \theta_j)} = a_8 \frac{w_{i,j,k+1} - w_{i,j,k}}{z_{k+1} - z_k} \tag{6}$$

$$2\frac{u_{i+1,j,k} r_{i+1} - u_{i,j,k} r_i}{(r_{i+1}^2 + r_i^2)} = -(1 - a_8)\frac{w_{i,j,k+1} - w_{i,j,k}}{z_{k+1} - z_k} \tag{7}$$

where $w_{i,j,k+1}$, $w_{i,j,k}$ are axial vertical velocities on the element boundaries between $z = z_{k+1}$ and $z = z_k$; $u_{i+1,j,k}$ and $u_{i,j,k}$ are radial vertical velocities on those between $r = r_{i+1}$ and $r = r_i$; $v_{i,j+1,k}$ and $v_{i,j,k}$ are circumferential vertical velocities on those between $\theta = \theta_{j+1}$ and $\theta = \theta_j$; a_8 is an optimization parameter determined through minimizing the total work of deformation in the process. Thus a kinematically admissible velocity field is established.

Applying the compatibility equation in cylindrical coordinates, the strain-rate field can be determined from the flow-velocity field determined above. On the basis of the upper-bound theorem, the total deformation power rate is given by

$$\dot{W} = Y \sum \int_V \sqrt{\frac{2}{3}\dot{\varepsilon}_{ij} \cdot \dot{\varepsilon}_{ij}} \mathrm{d}V + k \sum \int_t |\Delta v_t| \mathrm{d}t + mk \sum |\Delta v_f| \cdot F_f \quad (i, j = r, \theta, z) \tag{8}$$

where Y is the mean flow stress of the working material; k is the shearing resistance, $k = Y/\sqrt{3}$; m is the friction factor, $0 \leqslant m \leqslant 1$ ($m = 1$ being used in the calculation of this paper); Δv_t is the velocity discontinuity along tangent direction on the element boundaries and rigid-plastic boundaries; Δv_f is the relative slipping velocity on the interfaces between material and tools, and F_f being the area of the interfaces. The first term on the right-hand side of Eqn.(8) means the internal power rate of plastic deformation in element, the second means the shear power rate losses on the discontinuous velocity boundaries and the third the friction power rate losses over the interfaces between the tools and the material. Then the mean extrusion pressure is given by

$$p = \dot{W}/F_0 v_0 \tag{9}$$

3 RUSULTS AND DISCUSSION

In order to examine the reliability of the numerical model in this paper, the calculated extrusion pressure-stroke curve is compared with the results of experiment and UBA calculation given by Ref.[7]. The results show that the extrusion pressure calculated by UBET method is 0.5% ~ 5% greater than UBA calculated results and 5% ~ 15% greater than experimental results. So it is believable that the UBET model established in this paper is effective in simulation of the process of ribbed thin-wall pipe extrusion through a porthole die and the predicted extrusion pressure precise can meet the requirement of engineering application.

For the ribbed thin-wall pipe shown in Fig.1 (can also refered to Figs.2, 3, 4), the calculation conditions and calculated results are given in Table 1 and Table 2, respectively.

Table 2 shows that the calculated extrusion load is 22785 kN which is within the load capacity of practical extrusion pressure.

The depth of welding chamber (h) and the maximum opening angles ($\theta_{\max i}$) of plastic regions corresponded to portholes are the optimization parameters in the UBET model. Table 2 shows the extrusion pressure reaches a minimum when the depth of welding chamber (h) is 22.1 mm. The optimum depth of welding chamber, $h = 22.1$ mm is about 10% of the circumscribed diameter of portholes[4] and 2.1 mm greater than 20 mm taken by practical production.

Among four dividing deformation regions, that corresponded to the ribbed part of pipe has the maximum opening angle of deformation region, $\theta_{\max 1} = 0.703\pi$. It means that the metal flow through porthole ① is the maximum. The opposite of dividing deformation, the opening angle of the welding deformation region ①, $\theta'_{\max 1}$ corresponding with the ribbed part of the pipe is the minimum. Above results repre-

Table 1 Calculation conditions for extruding thin-wall pipe with one rib through a porthole die

Container diameter, D_c/mm	260	Width of rib head, B_f/mm	16.4
Outer radius of porthole, R_k/mm	120	Thickness of rib head, t_f/mm	2
Bottom outer radius of porthole for forming ribbed part, R_{kd}/mm	130	Height of rib, h_f/mm	2
Inner radius of porthole, R_x/mm	60	Thickness of rib, t_b/mm	2
Length of die land, l_d/mm	5.5	Velocity of extrusion ram/(mm•s^{-1})	1
Bridge width, B_b/mm	45	Extrusion temperature/ ℃	500
Inner diameter of pipe, d_m/mm	163	Mean flow stress of 6063, Y	14.7
Thickness of pipe, t/mm	1.4	Friction factor, m	1.0

Table 2 Calculated results with UBEF model

Dividing deformation region			Welding deformation region		
Area	$\theta_{\max i}$	$\theta_{\max i}$ value	Area	$\theta'_{\max i}$	$\theta'_{\max i}$ value
①	$\theta_{\max 1}$	0.703π	①	$\theta'_{\max 1}$	0.401π
② ④	$\theta_{\max 2}$, $\theta_{\max 4}$	0.380π	② ④	$\theta'_{\max 2}$, $\theta'_{\max 4}$	0.470π
③	$\theta_{\max 3}$	0.536π	①	$\theta'_{\max 3}$	0.659π
H_1/mm		23.7	h_1/mm		14.2
H_2/mm		20.1	h_2/mm		11.1
H_3/mm		20.9	h_4/mm		0.6
H_4/mm		12.1	Depth of welding chamber h/mm		22.1
Mean extrusion pressure p = 429.2 MPa					
Extrusion load p = 22 785 kN					

$\theta_{\max 1}$, $\theta'_{\max 1}$ represent maximum opening angle of dividing deformation region and welding deformation region corresponded to ribbed part of pipe, $\theta_{\max i}$ and $\theta'_{\max i}$(i = 2, 3, 4) represent those corresponded to other parts of pipe, subscript i is clockwise (refer to Fig. 6); h (h_3), h_1, h_2, h_4, H_1, H_2, H_3, H_4 are parameters describing shape of deformaion region (refer to Fig. 3 and Fig. 4)

sent the positions of dividing planes in the container are inconsistent with those of welding planes in welding chamber.

Fig. 6 shows the schematic drawing of four metal

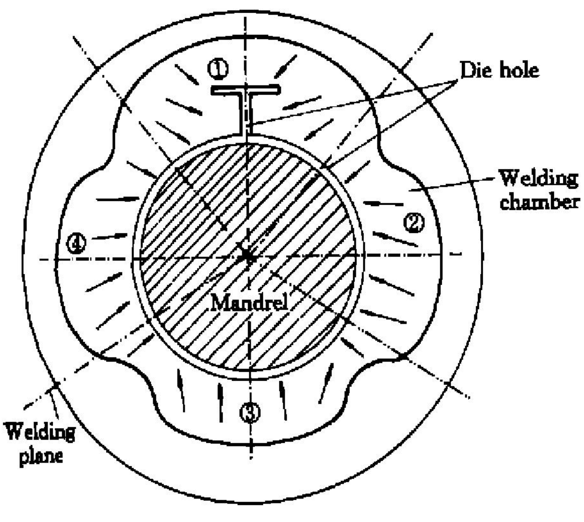

Fig. 6 Metal flow pattern in welding chamber

flow regions corresponding with four portholes in welding chamber according the results in Table 2. Four double dotted lines mean four welding planes. Because the opening angle of region ③ being maximum, there exits traverse metal flow on the whole in the welding chamber. Two types of product defects will be caused by this metal flow characteristic. One is product bend because of unequal flow out velocity, and another is unequal wall thickness in extruded pipe because of the bent deformation in mandrel. Therefore, to obtain more equitable metal flow in welding chamber, it is required to make the dividing planes $\theta_{\max i}$ to be consistent with corresponding welding planes $\theta_{\max i}$(i = 1, 2, 3, 4) through choosing different enter areas for each of the portholes.

Fig. 7 shows the relationship between extrusion pressure and extrusion ratio. The extrusion pressure is almost related linearly to extrusion raitio. The relationship can be given by

$$p/Y = 14.3 + 0.91R^{0.683} \tag{10}$$

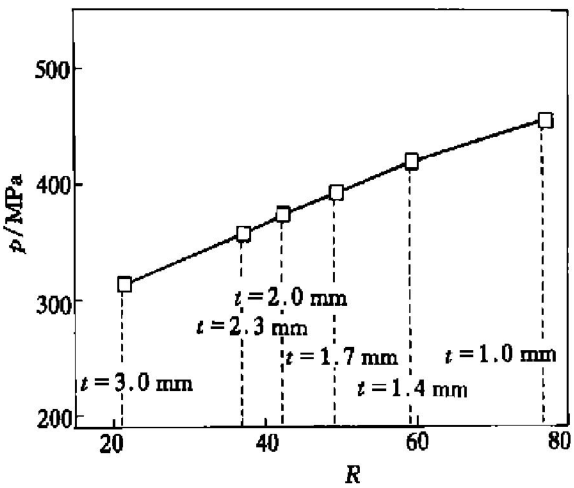

Fig. 7 Relationship between extrusion pressure (p) and exturusion ratio

(R defined as ratio of cross-sectional area of container to that of extruded pipe)

D_c = 260 mm, h = 22.1 mm, L_b/D_c = 1.923, Y = 14.7 MPa, m = 1.0, 4-hole, R_k = 120 mm, R_x = 60 mm, R_{kd} = 130 mm, d = 166.6 mm, t_f = t + 0.6 mm, h_f = t + 37.0 mm

Fig. 8 shows the relationship between extrusion pressure component p_d (required for the deformation in the dividing process), plastic region height H, and the billet length L_b in the container. When the billet length is greater than a quarter of the container diameter (i. e. $L_b \geqslant 1/4D_c$), the height of the plastic region H in the container remains almost constant and the extrusion pressure component p_d decreases along with the extrusion process goes on; when L_b is shorter than a quarter of the container diameter ($L_b < 1/4D_c$), however, the plastic region extends over the whole remained billet ($H/L_b = 1$) and the metal flow becomes unsteady which means that the extrusion process reaches the phase of funnel deformation, thus the extrusion pressure component p_d increases with extrusion stroke.

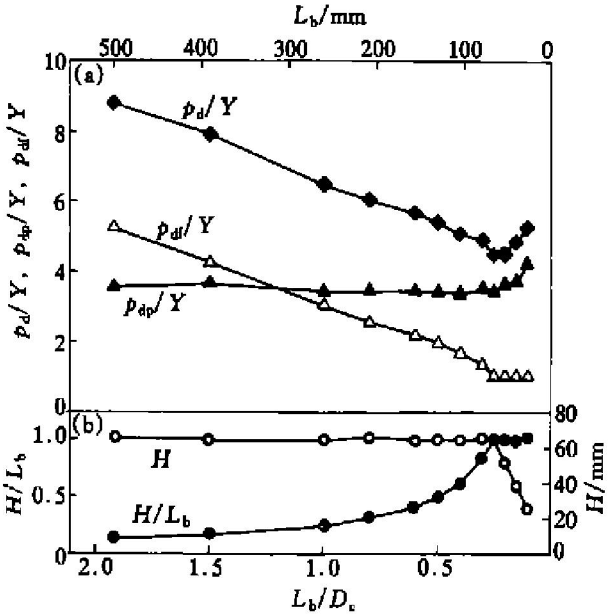

Fig. 8 Relationship between extrusion pressure component (p_d), plastic region height (H) and billet length (L_b) in container

($p_d = p_{dp} + p_{df}$, p_{dp} denotes component for internal plastic deformation and p_{df} for shear deformation on rigid-plastic boundary and friction on interfaces between working material and tools)

4-hole, $R_k = 120$ mm, $R_x = 60$ mm, $d_m = 163.8$ mm, $t = 1.4$ mm, $D_c = 260$ mm, $h = 22.1$ mm, $Y = 14.7$ MPa, $m = 1.0$, $B_b = 45$ mm

Fig. 9 shows the relationship between extrusion pressure (p), as well as the components (p_d, p_w) and the welding ratio (K, defined as the ratio of total entering area of portholes to that of extruded pipe). In the calculation, the number and the circumscribed diameter of portholes remains constant while the bridge width B_b and the inner radius R_x of portholes are changed in a certain proportion in calculation. With welding ratio K increased (bridge width B_b decreases), as shown in Fig. 9, the extrusion pressure component p_w required by deformation in welding region increases whilst the extrusion pressure component p_d required by deformation in dividing region decreases, and total extrusion pressure p ($p = p_w + p_d$) decreases slightly.

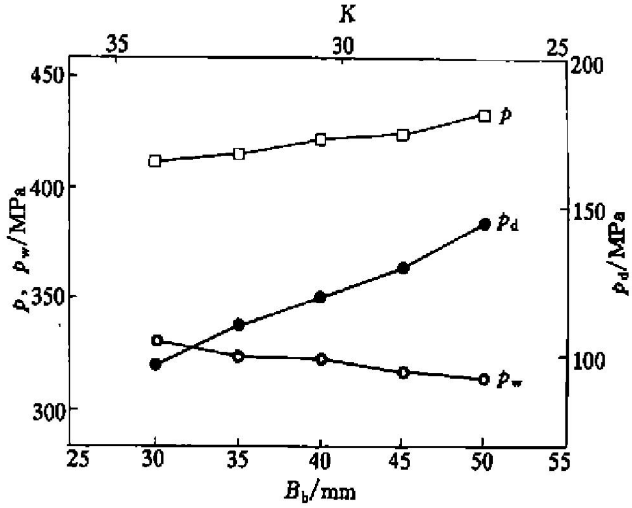

Fig. 9 Relationship between extrusion pressure (p) as well as components (p_d, p_w), and welding ratio (K) + means that strength of bridge is not enough

$D_c = 260$ mm, $h = 22.1$ mm, $R_k = 120$ mm,
$R_x = 60 - (45 - B_b)/2$, $d_m = 163.8$ mm, $t = 1.4$ mm,
$h_f = 38.4$ mm, $B_f = 46.4$ mm, $t_f = 2$ mm,
$L_b = 500$ mm,
$L_{pt} = 130$, $m = 1.0$,
$Y = 14.7$ MPa

[REFERENCES]

[1] Laue K, Stenger H. Extrusion (Processes, Machinery, Tooling) [M]. Ohio: American Society for Metals, 1981.

[2] LIU Jing-an. Extrusion Tooling and Dies for Light Metals [M], (in Chinese). Beijing: Metallurgical Industry Press, 1990.

[3] LIU Jing-an, KUANG Yong-xiang, LIANG Shi-bin, et al. Practical Techniques of Aluminium Alloy Profiles Production [M], (in Chinese). Chongqing: Chongqing International Information Advisory Center, 1994.

[4] XIE Jian-xin, LIU Jing-an. Theories and Technologies of Metal Extrusion [M], (in Chinese). Beijing: Metallurgical Industry Press, 2001.

[5] LIN Zhi-ping. Applications of Upper-Bound Theorem in Metal Forming [M], (in Chinese). Beijing: China Railway Industry Press, 1991.

[6] XIE Jian-xin, Ikeda K, Murakami T. Experimental simulation of metal flow in porthole-die extrusion [J]. J Mater Proc Tech, 1995, 49(1-2): 1-11.

[7] XIE Jian-xin, Ikeda K, Murakami T. UBA analysis of the process of pipe extrusion through a porthole die [J]. J Mater Proc Tech, 1995, 49(3-4): 371-385.

[8] XIE Jian-xin, Murakami T, Ikeda K, et al. Behavior of charge welding in porthole die extrusion [J]. J Japan Society for Technology of Plasticity, (in Japanese), 1995, 36(411): 390-395.

(Edited by HUANG Jin-song)